View metadata, citation and similar papers at core.ac.uk

brought to you by CO

provided by Elsevier - Publisher Conne

Journal of the American College of Cardiology
© 2000 by the American College of Cardiology
Published by Elsevier Science Inc.

Vol. 36, No. 6, 2000
ISSN 0735-1097/00/$20.00
PII S0735-1097(00)00960-8

Metabolism

Magnetic Resonance Spectroscopy Evidence of Abnormal Cardiac Energetics in Xp21 Muscular Dystrophy

Jenifer G. Crilley, MB, ChB, MRCP,*† Ernest A. Boehm, DPhil,†
Bheeshma Rajagopalan, MB, ChB, FRCP, DPhil,* Andrew M. Blamire, PhD,* Peter Styles, DPhil,*
Francesco Muntoni, MD, FRCPCH,‡ David Hilton-Jones, MD, FRCP,§ Kieran Clarke, PhD†
Oxford and London, United Kingdom

OBJECTIVES Our aim was to measure the cardiac phosphocreatine to adenosine triphosphate ratio (PCr/ATP) noninvasively in patients and carriers of Xp21 muscular dystrophy and to correlate the results with left ventricular (LV) function as measured by echocardiography.

BACKGROUND Duchenne and Becker muscular dystrophy (the Xp21 dystrophies) are associated with the absence or altered expression of dystrophin in cardiac and skeletal muscles. They are frequently complicated by cardiac hypertrophy and dilated cardiomyopathy. The main role of dystrophin is believed to be structural, but it may also be involved in signaling processes. Defects in energy metabolism have been found in skeletal muscle in patients with Xp21 muscular dystrophy. We therefore hypothesized that a defect in energy metabolism may be part of the mechanism leading to the cardiomyopathy of Xp21 muscular dystrophy.

METHODS Thirteen men with Becker muscular dystrophy, 10 female carriers and 23 control subjects were studied using phosphorus-31 magnetic resonance spectroscopy and echocardiography.

RESULTS The PCr/ATP was significantly reduced in patients (1.55 ± 0.37) and carriers (1.37 ± 0.25) as compared with control subjects (2.44 ± 0.33; $p < 0.0001$ for both groups). The PCr/ATP did not correlate with LV ejection fraction or mass index.

CONCLUSIONS Altered expression of dystrophin leads to a reduction in the PCr/ATP. Since this reduction did not correlate with indexes of left ventricular function, this raises the possibility of a direct link between altered dystrophin expression and the development of cardiomyopathy in such patients. (J Am Coll Cardiol 2000;36:1953–8) © 2000 by the American College of Cardiology

Duchenne muscular dystrophy (DMD) and Becker muscular dystrophy (BMD) are inherited neuromuscular disorders caused by an absence or decrease, respectively, in the cytoskeletal protein called dystrophin. Dystrophin is a large subsarcolemmal protein encoded by a gene at position 21 on the long arm of the X chromosome (Xp21).

Patients with DMD have progressive skeletal muscle weakness. Asymptomatic cardiac involvement is widespread by the time patients reach their early teens, with 80% having an abnormal electrocardiogram (ECG) echocardiogram, or both (1). Skeletal muscle weakness remains the primary limiting symptom, and this may explain why patients remain asymptomatic from such cardiac involvement, even late in the course of their disease. As the respiratory component of patients' symptoms is becoming more widely treated (2), it is likely that recognition and management of the cardiac component will assume greater importance.

From the *Biochemical and Clinical Magnetic Resonance Unit, John Radcliffe Hospital, Oxford, United Kingdom; †BHF Molecular Cardiology Group, Department of Biochemistry, University of Oxford, South Parks Road, Oxford, United Kingdom; ‡Department of Pediatrics and Neonatal Medicine, Imperial College of Medicine, Hammersmith Campus, London, United Kingdom; and §Muscle and Nerve Centre, Radcliffe Infirmary, Oxford, United Kingdom. The study was funded by the British Heart Foundation and the Medical Research Council.

Manuscript received December 20, 1999; revised manuscript received May 30, 2000; accepted July 14, 2000.

In contrast, skeletal muscle weakness is milder in BMD. Symptomatic cardiomyopathy may dominate the clinical picture and is thought to be the leading cause of death in such patients (3). Asymptomatic cardiac involvement in the form of ECG and transthoracic echocardiographic (TTE) abnormalities affects from 15% of patients <16 years old to 70% of patients >40 years old (4).

Several studies have also demonstrated subclinical cardiac involvement in female carriers of DMD. Although ECG or TTE abnormalities are present in up to 40% of individuals (5,6), clinical symptoms directly attributable to cardiomyopathy are comparatively rare, arising in ~5% of carriers (7).

Histologic evidence suggests that the characteristic skeletal muscle dystrophic changes of the Xp21 dystrophies are also present in the heart (8), including patchy dystrophin staining in heart biopsies of patients with BMD (9).

Phosphorus-31 magnetic resonance spectroscopy (^{31}P-MRS) is a noninvasive technique that allows the in vivo detection of high energy phosphate–containing metabolites. Cardiac ^{31}P-MRS enables determination of the phosphocreatine to adenosine triphosphate ratio (PCr/ATP), which is an indicator of the energetic state of cardiac muscle (10). The ^{31}P-MRS studies in patients with DMD and BMD and in female carriers have shown a reduced PCr/ATP in skeletal muscle (11,12). In view of these findings and the

JACC Vol. 36, No. 6, 2000
November 15, 2000:1953–8

Abbreviations and Acronyms

1D-CSI	=	one-dimensional chemical shift imaging
BMD	=	Becker muscular dystrophy
DMD	=	Duchenne muscular dystrophy
FID	=	free induction decay
LV	=	left ventricular
PCr/ATP	=	phosphocreatine to adenosine triphosphate ratio
^{31}P-MRS	=	phosphorus-31 magnetic resonance spectroscopy
TE	=	echo time
TR	=	relaxation time
TTE	=	transthoracic echocardiogram

similar histologic findings in heart and skeletal muscle, we used ^{31}P-MRS to investigate cardiac energetics in patients with and carriers of Xp21 muscular dystrophy.

METHODS

Subjects. Potential participants in the study were identified from a data base held by the Regional Genetics Service, Churchill Hospital, Oxford, United Kingdom. Thirteen men (mean age 30 years [range 12 to 48]) with BMD and 10 female carriers from families with DMD (mean age 46 years [range 26 to 62]) volunteered to take part in the study. A diagnosis of BMD was made by the identification of a mutation in the dystrophin gene (n = 10) or by abnormal dystrophin immunohistochemical staining on muscle biopsy (n = 3), or both. Carrier status was confirmed either by DNA analysis (n = 8) or by the presence of a family pedigree, indicating that the participant may be an obligate carrier (n = 2). All subjects were examined and classified into four functional groups: 1 = raised serum creatine kinase but otherwise asymptomatic; 2 = symptomatic but able to rise from a chair and climb stairs unaided; 3 = ambulant but not able to climb stairs or rise from a chair unaided; and 4 = wheelchair-bound. Two patients and eight carriers were in class 1; five patients and one carrier were in class 2; three patients and one carrier were in class 3; and three patients were in class 4. Two carriers were thus classified as manifesting carriers. Subjects had TTE and ^{31}P-MRS of the heart performed. A similar number of age- and gender-matched volunteers (12 men, mean age 32 years [range 17 to 45]; 11 women; mean age 41 years [range 29 to 61]) were also studied by ^{31}P-MRS only. These volunteers were free of symptoms or signs of cardiovascular or neuromuscular disease and were not taking any cardioactive treatments. All subjects gave written consent, and the study was approved by the Central Oxford Research Ethics Committee.

Cardiac ^{31}P-MRS. SPECTRAL ACQUISITION. Patients were studied using a 2-tesla whole-body magnet (Oxford Magnet Technology, Oxford, United Kingdom), which was interfaced to a Bruker Avance spectrometer (Bruker Medical GmbH, Ettlingen, Germany). Patients were examined at rest and lay prone on a custom-designed bed incorporating a gantry that allowed a range of surface coils to be positioned beneath the precordium without moving the subject. Patients were positioned with their heart at the isocenter of the magnet, and this was confirmed using standard multislice spin-echo proton images acquired using a double-rectangular surface coil placed around the chest (relaxation time [TR] = heart rate, echo time [TE] = 25 ms, slice = 10 mm, 5 slices, 15-mm spacing). These images were also used to verify that the diaphragm would not be within the field of view during the ^{31}P acquisition. The imaging coil was exchanged for a circular proton surface coil (15-cm diameter) placed beneath the chest, and shimming was performed to optimize the magnetic field homogeneity over the heart. Finally, the coil was exchanged for a ^{31}P surface coil (8-cm diameter). To ensure full localization of the ^{31}P-MRS data to the heart, spectra were acquired using a slice-selective, one-dimensional chemical shift imaging (1D-CSI) sequence, including spatial presaturation of lateral skeletal muscle, as follows. An oblique-angled saturation slab was positioned from the proton images across any skeletal muscle lateral to the surface coil, and all ^{31}P signals were saturated using two pairs of sinc pulses at a 1:2 flip/angle ratio (13). An 8-cm thick transverse slice was then excited, followed by one-dimensional phase encoding into the chest to subdivide signals into 64 coronal layers, each 1-cm thick (TR = heart rate, 16 averages). All proton and ^{31}P data at acquisition were cardiac gated using a pulse oximeter probe placed on the subject's finger.

SATURATION CORRECTION. The interpulse delay (TR) for the 1D-CSI data set, which is determined by the heart rate, is much shorter than the T1 relaxation times for ATP and PCr. This leads to a reduction in measured signal intensity, which is a function of the pulse angle, repetition rate and the different T1 relaxation times of the metabolites. To allow for this effect, saturation correction factors were measured by obtaining 1D-CSI spectra from ^{31}P phantoms of known T1 relaxation times at different repetition rates. The ionic strengths of the phantom were adjusted so that the pulse angle at the surface of the coil was similar for equivalent power levels for both phantoms and human subjects. The T1 relaxation times of PCr and ATP were assumed to be 4.3 s and 2.5 s, respectively, these being the average of published data (14).

As the magnitude of the correction factors is very sensitive to the assumed T1 relaxation times, both the raw and corrected ratios are presented in this report. It should be noted, when comparing the corrected data from different investigators, that there are several strategies for making this saturation correction. The difference between the correction factors for heart rates of 55 and 100 beats/min is only 4% to 5%. Thus, although the corrected PCr/ATP from different reports may vary, the correction factor has little effect on the relative differences between patients and control subjects, as reported here.

Table 1. Echocardiographic Features of Patients and Carriers*

	ESD (cm)	EDD (cm)	IVSd (cm)	PWd (cm)	LVMI (g/m$^{2.7}$)	EF
Patient						
1	3.64	4.94	0.73	0.60	40.3	0.54
2	4.23	5.00	0.66	0.51	25.8	0.42
3	4.19	5.13	0.84	0.72	30.1	0.41
4	3.22	4.87	0.96	0.87	41.1	0.48
5	3.90	5.29	0.87	0.78	35.6	0.43
6	4.92	5.68	1.03	0.69	42.6	0.35
7	4.14	5.59	0.77	0.67	31.9	0.35
8	3.33	5.00	0.94	1.03	48.9	0.51
9	3.74	4.14	1.12	1.12	42.2	0.52
10	3.04	4.98	0.72	0.72	25.1	0.62
11	3.68	5.19	0.85	0.85	33.1	0.59
12	2.74	4.81	1.25	1.04	49.7	0.56
13	3.12	4.83	0.71	0.93	33.6	0.59
Mean ± SD	3.7 ± 0.6	5.0 ± 0.4	0.88 ± 0.17	0.81 ± 0.18	37 ± 7.9	0.49 ± 0.09
Carriers						
1	4.44	5.82	0.94	0.81	57.8	0.50
2	3.40	4.27	0.76	0.55	25.5	0.50
3	3.39	4.79	0.89	0.89	35.6	0.57
4	3.17	4.72	0.71	0.6	24.5	0.51
5	3.51	5.14	0.57	0.85	39.2	0.65
6	4.50	5.65	0.9	0.74	45.1	0.54
7	3.65	5.77	0.61	0.79	37.6	0.62
8	3.18	4.88	0.85	0.9	41.7	0.51
9	2.70	5.03	1.05	1.11	60.5	0.63
10	3.14	4.63	0.86	0.86	41.2	0.53
Mean ± SD	3.5 ± 0.6	5.0 ± 0.5	0.81 ± 0.15	0.81 ± 0.16	41 ± 12	0.56 ± 0.06

*Carriers 9 and 10 were manifesting carriers.

EDD = end-diastolic diameter; EF = ejection fraction; ESD = end-systolic diameter; IVSd = interventricular septal thickness in diastole; LVMI = left ventricular mass index (upper limit of normal = 51 g/m$^{2.7}$ for males and 48 g/m$^{2.7}$ for females); PWd = posterior wall thickness in diastole.

DATA PROCESSING. The proton images were used to determine those spectra in the cardiac 1D-CSI data set that arose from the myocardium. Spectral data were Fourier-transformed, with 15 Hz of line broadening applied. The cardiac rows with an acceptable signal to noise ratio were extracted for analysis, and rows with a similar morphology were added. The row immediately adjacent to the chest wall was not analyzed to avoid contamination from residual skeletal muscle signal. Spectra were fitted using a purpose-designed interactive frequency domain-fitting program similar to one recently described (15). Time-domain signals were simulated for PCr, the three peaks of ATP, phosphodiesters and 2,3-diphosphoglycerate by incorporating previous knowledge of peak chemical shifts and *J* couplings. Each signal component was simulated allowing for missing data points (due to the phase-encoding duration of the acquisition experiment). Signal amplitude and exponential decay of each component was adjustable, and gaussian decay could be applied to the whole free induction decay (FID). The simulated FID was Fourier-transformed. The root mean square residual between the simulated and acquired spectrum was calculated as a measure of the fit. After fitting, the ATP signal was corrected for blood contamination according to the amplitude of the 2,3-diphosphoglycerate signal (16–18), and the PCr/ATP was calculated. The calculated PCr/ATP was corrected for magnetic saturation effects (as described earlier).

Echocardiography. Echocardiography was performed by the same operator (J.G.C.) in all patients, using a SONOS 5500 (Hewlett-Packard, Bracknell, United Kingdom), and images were stored on videotape or optical disk for later analysis. Left ventricular dimensions were obtained using M-mode echocardiography; ejection fraction was calculated, when possible, from LV volumes (derived using the modified Simpson's rule); and diastolic function was evaluated by acquisition of a pulsed Doppler recording trace through the mitral valve, with the sample volume positioned just above the mitral valve tips. Left ventricular mass index was derived from M-mode echocardiographic measurements using the Wikstrand formula (19), which uses a modification of the prolate ellipsoid geometric assumption of LV morphology, and was adjusted for height, as recommended by de Simone et al. (20).

Statistical analysis. The PCr/ATP data, comparing the patient and carriers with their respective control subjects, were analyzed using the Mann-Whitney *U* test, and echocardiographic data were analyzed using the Student *t* test. Results are reported as the mean value ± SD. Statistical significance was taken as $p < 0.05$.

RESULTS

Echocardiography. The results of TTE in the patient and carrier groups are summarized in Table 1. Mild TTE

JACC Vol. 36, No. 6, 2000
November 15, 2000:1953–8

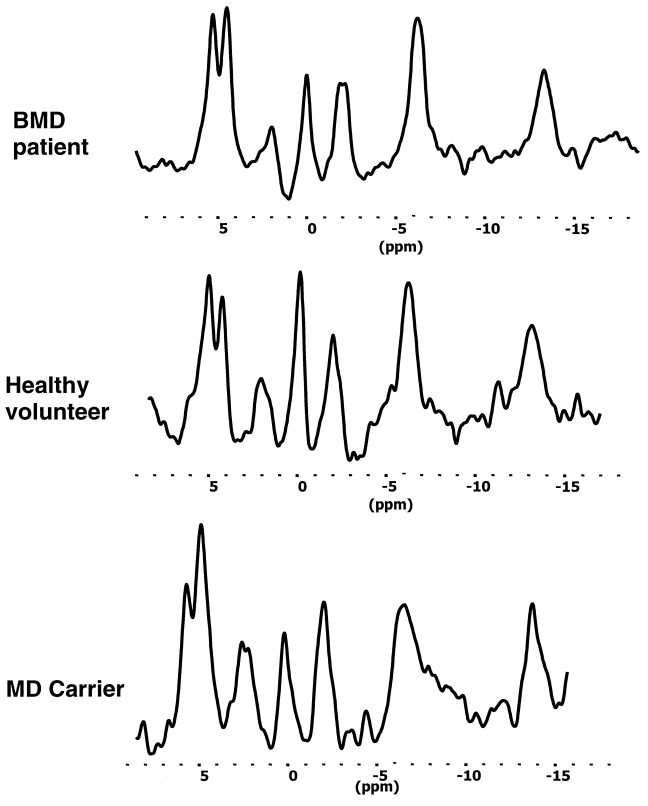

Figure 1. Examples of spectra from a patient with BMD, a female carrier of muscular dystrophy (MD) and a healthy volunteer.

abnormalities were common among both cohorts of patients with BMD and DMD carriers. No patient or carrier had clinical symptoms or signs of heart failure. An ejection fraction <50% was present in 46% of the patient cohort. Only one patient with BMD, the youngest, had a completely normal echocardiogram. None of the carriers had an ejection fraction <50%. Two carriers (one manifesting) had an increase in LV mass index, but neither had objective evidence of associated diastolic dysfunction. The mean ejection fraction was significantly lower in the patient cohort than in the carrier cohort (49 ± 9% vs. 56 ± 6%, $p < 0.05$). However, there were no other significant differences in the other echocardiographic variables.

^{31}P-MRS data. Examples of cardiac spectra acquired from a patient with BMD, a healthy volunteer and a DMD carrier are shown in Figure 1. The PCr/ATP (uncorrected for saturation) was significantly lower in the patients with BMD as compared with the male control subjects (1.15 ± 0.27 vs. 1.92 ± 0.22, $p < 0.001$). It was also significantly lower in the DMD carriers as compared with the female control subjects (1.14 ± 0.20 vs. 1.89 ± 0.28, $p < 0.001$). This difference remained significant after correction for saturation effects (1.55 ± 0.37 vs. 2.49 ± 0.31, $p < 0.001$, and 1.37 ± 0.25 vs. 2.38 ± 0.36, $p < 0.001$, respectively [Fig. 2]). There was no correlation between the PCr/ATP and any echocardiographic indexes of LV function.

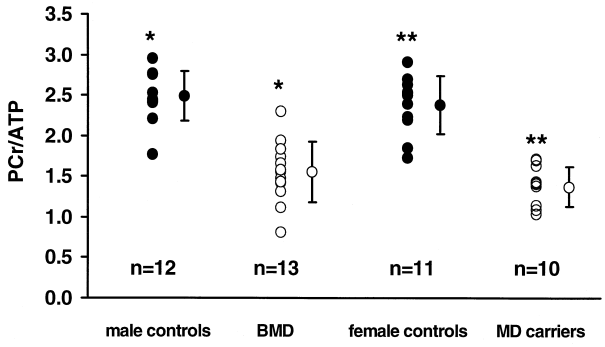

Figure 2. Results of saturation-corrected PCr/ATP for patients with BMD and carriers of muscular dystrophy (MD) as compared with control subjects. * and **$p < 0.0001$.

DISCUSSION

In this study, we have shown, using ^{31}P-MRS, that cardiac energy metabolism is abnormal in both patients with and carriers of Xp21 muscular dystrophy. A significant reduction in the PCr/ATP was found in both subject groups as compared with control groups. The magnitude of this reduction was similar for both the patient and carrier cohorts. The ratios were also similar between the manifesting and nonmanifesting carriers. The presence of a reduced PCr/ATP in the absence of either LV systolic or diastolic dysfunction or an increase in LV wall thickness implies that cardiac metabolic dysfunction in Xp21 muscular dystrophy precedes the deterioration of LV function, and is not a result of it. Our results are in contrast to most previous studies of cardiac energetics in heart failure and cardiac hypertrophy, which have shown a distinct correlation between a reduction in the PCr/ATP and indexes of LV function (16–18).

Phosphocreatine is an important metabolite in the biochemical pathways that supply ATP for muscle contraction. Phosphocreatine can rapidly phosphorylate adenosine diphosphate (ADP) to ATP through the creatine kinase reaction, which is believed to be at equilibrium. Thus, PCr buffers the concentration of ATP during sudden demands in energy requirements, regulates ADP (a controller of oxidative metabolism) and may also have a role in transferring high energy phosphates from the mitochondria to the myofibrils (the creatine kinase shuttle) (21).

Several studies have shown alterations in cardiac energetics in various forms of cardiomyopathy and heart failure. Lamb et al. (22) have reported a reduction in the PCr/ATP in patients with cardiac hypertrophy secondary to essential hypertension, the magnitude of which correlated with indexes of diastolic dysfunction. Studies of valvular heart disease have also demonstrated reductions in the PCr/ATP, which appeared to correlate with measures of systolic LV dysfunction (16). These studies have indicated that changes in cardiac high energy phosphate metabolism are associated with increased mechanical loading of the heart.

The cause of the reduced PCr/ATP in these studies is

unclear, but several mechanisms may be important. First, isolated perfused hearts have a lower PCr/ATP when glucose is the sole substrate (23). Although shifts toward increased glucose utilization have been found in rat models of cardiac hypertrophy (24), it would seem unlikely that the human heart would alter its metabolism to a sufficient extent to produce such a pronounced fall in PCr/ATP, as we found in our study. Second, severely compromised oxygen delivery to the heart leads to anaerobic ATP production, and decreased PCr/ATP has been found in animal hearts subjected to ischemia (25). Again, this situation is unlikely to exist in the human heart, other than in myocardial regions supplied by an occluded coronary artery, and would not account for major reductions in PCr/ATP under states of adequate oxygen delivery at rest. Third, an increase in cardiac work load (through volume or pressure loading) could decrease PCr/ATP. Evidence for this is conflicting, with some studies showing preserved PCr/ATP with increased cardiac work load (26), and others showing a small fall (5% to 10%) in PCr/ATP with dobutamine–atropine stress (27). It seems unlikely that a moderate increase in work load (i.e., a level induced by normal daily activity) would cause a sustained fall in PCr/ATP, because increased mitochondrial ATP production and improved oxygen delivery would more than compensate, thus suggesting that other mechanisms are responsible for the perturbations in energetics in heart failure. However, intrinsic defects of mitochondrial function due to mutations affecting respiratory chain enzymes could impair this response. We have recently found a reduced PCr/ATP in the heart of patients with the mitochondrial encephalopathy, lactic acidosis and stroke-like episodes (MELAS) syndrome in the absence of defects of LV systolic function (28).

In this study, we found no relationship between the PCr/ATP and indexes of systolic or diastolic function. The ratio was uniformly reduced to an equal extent among those with both normal and abnormal LV function. This raises two intriguing questions. First, what is the cause of the low PCr/ATP in our patients and carriers? Second, does the PCr/ATP have any relationship to the pathophysiologic mechanisms of cardiomyopathy in Xp21 muscular dystrophy?

Cause of reduced PCr/ATP. Because there was no evidence of increased afterload or reduced oxygen delivery in our subject group, alternative mechanisms must be considered. Although there is some evidence (29) for a decrease in respiratory chain complex activity in Xp21 muscular dystrophy (*mdx* mouse), other studies have suggested that mitochondrial function is not severely impaired (12), and thus it seems unlikely that this would account for our results.

The most likely explanation for our findings is a reduction in creatine. Two studies have shown a reduction in creatine content in human cardiomyopathies (30,31), when measured in vitro from cardiac biopsy specimens, and there are similar findings in animal models of myocardial infarction (32) and heart failure (33). In vivo support for this data has been described by Bottomley et al. (34), who found, using proton MRS, a reduction in the creatine content in infarct-related regions of human myocardium. A reduction in creatine, through the creatine kinase reaction—creatine + ATP $\leftrightarrow$ ADP + H^+ + PCr—leads to a fall in PCr, as long as the ratio (ADP)(H^+)/(ATP) remains constant. Recent evidence in a dog pacing model of heart failure suggests that there is a rise in this ratio due to a 20% reduction in ATP in advanced heart failure (33). In the same study, a fall in creatine of 41% was found, suggesting that a reduction in PCr/ATP is predominantly due to loss of creatine.

Relationship to pathophysiology of cardiomyopathy in Xp21 muscular dystrophy. The most important function of dystrophin appears to be membrane stabilization, although other properties such as linkage of force transduction between the intracellular and extracellular environments may contribute to the clinical phenotype of dystrophin deficiency (35). Ortiz-Lopez et al. (36) postulated that a failure to stabilize the membrane, particularly during repeated contraction of the heart, could lead to long-term loss of muscle integrity and cardiomyopathy. This reduction in membrane integrity may increase leakage of intracellular metabolites essential for muscle contraction, such as creatine. Thus, an energetic abnormality may be an important contributing mechanism leading to progression of cardiomyopathy in patients with DMD and BMD. Dystrophin may also be involved in the regulation of ion channels, such as the sodium-dependent membrane-bound creatine transporter, and alteration in localization or function of this transporter may lead to decreased intracellular creatine. Disruption of actin binding and interference with calcium regulation (37) may increase ATP turnover and exacerbate the deficiency of PCr. Studies in animal models of muscular dystrophy may help unravel these additional potential mechanisms.

Given that the spectra from the skeletal muscle, diaphragm and myocardium all contain peaks from PCr and ATP, the potential for contamination of cardiac signal from the surrounding tissue must be considered when interpreting our results. We used image-guided placement of a relatively small surface coil in conjunction with slice-selective acquisition to minimize contributions from the diaphragm. Slice selection is widely used in magnetic resonance imaging and is known to have high selectivity (>99%); thus, the potential for contamination from the diaphragm is minimal. Phantom data (unpublished) show that the phase-encoding scheme used to encode spectra with depth into the chest shows no cross-contamination of spectra from compartments that are separated by >5 mm. In our analysis, there was always at least one row (10 mm) between spectral rows containing skeletal muscle signal from the anterior chest wall and the row(s) assigned to myocardium. Thus, contamination from the chest wall, we believe, was also minimal.

Furthermore, previous studies from our institution, which has investigated phosphorus metabolites in the skeletal

muscle of patients with BMD (11,12), have shown a reduction in the PCr/ATP of 15% between patients and control subjects. We also analyzed the PCr/ATP in the skeletal muscle row of the cardiac data set in our patients, carriers and control subjects, and we found a 17% reduction in PCr/ATP between the patient and carrier groups and control group. Our results suggest that it is unlikely that skeletal muscle contamination of the cardiac signal could account for the 38% to 42% reduction in cardiac PCr/ATP that we found between our patients with BMD and DMD carriers and control subjects.

There is much controversy as to whether abnormalities of cardiac energetics are the cause or the consequence of cardiac hypertrophy and heart failure. The consistent finding in our study of reduced PCr/ATP, which did not correlate with ejection fraction or LV mass index, adds further weight to the hypothesis that an abnormality of cardiac energetics is important in the etiology of cardiomyopathy in Xp21 muscular dystrophy. Furthermore, knowledge of the mechanism by which a loss of dystrophin leads to cardiomyopathy may increase our understanding of the pathophysiologic mechanisms behind the development of cardiac failure in other cardiomyopathies.

Reprint requests and correspondence: Dr. J. G. Crilley, Biochemical and Clinical Magnetic Resonance Unit, John Radcliffe Hospital, Headley Way, Oxford, OX3 9DU, United Kingdom. E-mail: jcrilley@bioch.ox.ac.uk.

REFERENCES

1. Nigro G, Comi LI, Politano L, Bain RJI. The incidence and evolution of cardiomyopathy in Duchenne muscular dystrophy. Int J Cardiol 1990;26:271–7.
2. Simonds AK, Muntoni F, Heather S, Fielding S. Impact of nasal ventilation on survival in hypercapnic Duchenne muscular dystrophy. Thorax 1998;53:949–52.
3. Cox GF, Kunkel LM. Dystrophies and heart disease. Curr Opin Cardiol 1997;12:329–43.
4. Nigro G, Comi L, Politano L, et al. Evaluation of cardiomyopathy in Becker muscular dystrophy. Muscle Nerve 1995;18:283–91.
5. Mirabella M, Servidei S, Manfredi G, et al. Cardiomyopathy may be the only clinical manifestation in female carriers of Duchenne muscular dystrophy. Neurology 1993;43:2342–5.
6. Politano L, Vincenzo N, Nigro G, et al. Development of cardiomyopathy in female carriers of Duchenne and Becker muscular dystrophies. JAMA 1996;275:1335–8.
7. Hoogerwaard EM, Bakker E, Ippel PF, et al. Signs and symptoms of Duchenne muscular dystrophy and Becker muscular dystrophy among carriers in the Netherlands: a cohort study. Lancet 1999;353:2116–9.
8. Cohen S. Myocardial fibrosis in progressive muscular dystrophy. J Med 1936;17:26.
9. Anan R, Higuchi I, Ichinari K, et al. Myocardial patchy staining of dystrophin in Becker's muscular dystrophy associated with cardiomyopathy. Am Heart J 1992;123:1088–9.
10. Radda GK. The use of NMR spectroscopy for the understanding of disease. Science 1986;233:640–5.
11. Kemp GJ, Taylor DJ, Dunn JF, Frostick SP, Radda GK. Cellular energetics of dystrophic muscle. J Neurosci 1993;116:201–6.
12. Lodi R, Kemp GJ, Muntoni F, et al. Reduced cytosolic acidification during exercise suggests defective glycolytic activity in skeletal muscle of patients with Becker muscular dystrophy: an in vivo ^{31}P magnetic resonance spectroscopy study. Brain 1999;122:121–30.
13. Blamire AM, Rajagopalan B, Radda GK. Measurement of myocardial pH by saturation transfer in man. Magn Reson Med 1999;41:198–203.
14. Bottomley PA, Hardy CJ, Roemer PB. Phosphate metabolite imaging and concentration measurements in human heart by nuclear magnetic resonance. Magn Reson Med 1990;14:425–34.
15. Slotboom J, Boesch C, Kreis R. Versatile frequency domain fitting using time domain models and prior knowledge. Magn Reson Med 1998;39:899–911.
16. Conway MA, Bottemley PA, Ouwerkerk R, Radda GK, Rajagopalan B. Mitral regurgitation: impaired systolic function, eccentric hypertrophy and increased severity are linked to a lower phosphocreatine/ATP ratios in humans. Circulation 1998;97:1716–23.
17. Conway MA, Allis J, Ouwerkerk R, et al. Detection of low phosphocreatine to ATP ratio in failing hypertrophied human myocardium by ^{31}P magnetic resonance spectroscopy. Lancet 1991;338:973–6.
18. Hardy CJ, Weiss RG, Bottemley PA, Gerstenblith G. Altered myocardial high-energy metabolites in patients with dilated cardiomyopathy. Am Heart J 1991;122:795–801.
19. Wikstrand J. Calculation of left ventricular mass in man—a comment. J Hypertens 1997;15:811–3.
20. de Simone G, Daniels SR, Devereux R, et al. Left ventricular mass and body size in normotensive children and adults: assessment of allometric relations and impact of overweight. J Am Coll Cardiol 1992;20:1251–60.
21. Wallimann T, Wyss M, Brdiczka D, Nicolay K, Eppenberger HM. Intracellular compartmentation, structure, and function of creatine kinase isoenzymes in tissues with high and fluctuating energy demands: the phosphocreatine circuit for cellular energy homeostasis. Biochem J 1992;281:21–40.
22. Lamb HJ, Beyebacht HP, van der Laarse A, et al. Diastolic dysfunction in hypertensive heart disease is associated with altered myocardial metabolism. Circulation 1999;99:2261–7.
23. From AHL, Zimmer SD, Michurski SP, et al. Regulation of oxidative phosphorylation in the intact cell. Biochemistry 1990;29:3731–43.
24. Kayaga Y, Kanno Y, Takeyama D, et al. Effects of long-term pressure overload on regional myocardial glucose and free fatty acid uptake in rats: a quantitative autoradiographic study. Circulation 1990;81:1353–61.
25. Clarke K, Sunn I, Willis RJ. ^{31}P-NMR spectroscopy of hypertrophied rat heart: effect of graded global ischaemia. J Mol Cell Cardiol 1989;21:1315–25.
26. Schaefer S, Schwartz GG, Steinman SK, et al. Metabolic response of the heart to inotropic stimulation: in vivo phosphorus-31 studies of normal and cardiomyopathic myocardium. Magn Res Med 1992;25:260–72.
27. Lamb HJ, Beyerbacht HP, Ouwerkerk R, et al. Metabolic response of normal human myocardium to high-dose atropine-dobutamine stress studied by ^{31}P-MRS. Circulation 1997;96:2969–77.
28. Lodi R, Rajagopalan B, Blamire A, et al. Abnormal cardiac energetics measured in vivo by ^{31}P magnetic resonance spectroscopy in the MELAS syndrome (abstr). Eur J Cardiol 1999;20:2538.
29. Kuznetsov A, Winkler K, Wiedemann FR, et al. Impaired mitochondrial oxidative phosphorylation in skeletal muscle of the dystrophin-deficient *mdx* mouse. Mol Cell Biochem 1998;183:87–96.
30. Nescimben L, Ingwall JS, Pauletto P, et al. Creatine kinase system in failing and nonfailing human myocardium. Circulation 1996;94:1894–901.
31. Ingwall JS, Kramer MF, Kramer BA, et al. The creatine kinase system in normal and diseased human myocardium. N Engl J Med 1985;313:1050–4.
32. Neubauer SN, Horn M, Naumann A, et al. Impairment of energy metabolism in intact residual myocardium of rat hearts with chronic myocardial infarction. J Clin Invest 1995;95:1092–100.
33. Weiqun S, Kuniya A, Masami U, et al. Progressive loss of myocardial ATP due to a loss of total purines during the development of heart failure in dogs. Circulation 1999;100:2113–8.
34. Bottomley PA, Weiss RG. Noninvasive magnetic resonance detection of creatine depletion in nonviable infarcted myocardium. Lancet 1998;351:714–8.
35. Carlsen CG. The dystrophinopathies: an alternative to the structural hypothesis. Neurobiol Dis 1998;5:3–15.
36. Ortiz-Lopez MS, Hua L, Su J, et al. Evidence for a dystrophin missense mutation as a cause of X-linked dilated cardiomyopathy. Circulation 1997;95:2434–40.
37. Song KS, Scherer PE, Tang Z, et al. Expression of caveolin-3 in skeletal, cardiac and smooth muscle cells. J Biol Chem 1996;271:15160–5.